

Stability Analysis of Unsteady Ablation Fronts

R. Betti, R. L. McCrory, and C. P. Verdon

Laboratory for Laser Energetics, University of Rochester, 250 East River Road, Rochester, New York 14623-1299

(Received 22 June 1993)

The linear stability analysis of unsteady ablation fronts is carried out for a semi-infinite uniform medium. For a laser accelerated target, it is shown that a properly selected modulation of the laser intensity can lead to the dynamic stabilization or growth-rate reduction of a large portion of the unstable spectrum. The theory is in qualitative agreement with the numerical results obtained by using the two-dimensional hydrodynamic code ORCHID.

PACS numbers: 52.35.Py, 52.40.Nk

The classical Rayleigh-Taylor instability [1] occurs when a heavy fluid is accelerated by a lighter fluid. In inertial confinement fusion (ICF) the heavy fluid is the compressed ablated target material that is accelerated by the low-density ablated plasma. The classical treatment of the incompressible Rayleigh-Taylor instability leads to a linear growth rate given by $\gamma = \sqrt{|kg|A}$, where k is the instability wave number, g is the acceleration, and A is the Atwood number $A = (\rho_h - \rho_l)/(\rho_h + \rho_l)$ (ρ_l and ρ_h represent the light and heavy fluid densities, respectively). For typical (ICF) parameters a classical Rayleigh-Taylor instability would produce an unacceptably large amount of distortion in the unablated target, resulting in a degraded capsule performance with respect to the final core conditions. Thus, it is important to study the possible means for suppression of the ablation surface instability in ICF. It has been recently shown that the ablation process leads to convection of the perturbation away from the interface between the two fluids [2-5]. Since the instability is localized at the interface, the ablative convection stabilizes short wavelength modes. The typical growth rate of the ablative Rayleigh-Taylor instability can be written in the following approximate form [3]:

$$\gamma = \sqrt{|kg|A} - \beta |kV_a|, \quad (1)$$

where V_a is the ablation velocity and β is a numerical factor ($\beta \approx 3-4$).

In this paper we show that a properly selected modulation of the laser intensity can significantly reduce the unstable spectrum and the maximum growth rate. To treat the analytic linear stability of unsteady ablation fronts, we consider a simplified sharp boundary model consisting of a heavy fluid, with density ρ_h , adjacent to a lighter fluid (ρ_l), in the force field $\mathbf{g}(t) = g(t)\mathbf{e}_y$ in a direction opposite to the density gradient [$g(t) < 0$ and \mathbf{e}_y is the unit vector in the direction of the density gradient] and with an arbitrary time dependence. The heavy fluid is moving downward with velocity $\mathbf{U}_h = -V_a\mathbf{e}_y$ and the lighter fluid is ejected with velocity U_l . The equilibrium velocities $U_l(t)$ and $U_h(t)$ are both dependent on the ablation ratio per unit surface $\dot{m}(t)$, that is, treated as an arbitrary function of time. The equilibrium can be readily derived from conservation of mass and momentum. We consider a class of equilibria with nonuniformities lo-

calized at the interface between the two fluids. Continuity of the mass flow and the pressure balance across the interface lead to the following conditions:

$$\rho_l U_l(t) = \rho_h U_h(t), \quad (2)$$

$$P_h - P_l = \rho_l U_l^2(t) - \rho_h U_h^2(t), \quad (3)$$

where P_h and P_l represent the pressure of the heavy and light fluid, respectively, at the interface. Notice that U_l and U_h are negative in the chosen frame of reference. We assume that the discontinuities in the equilibrium quantities can be removed by including the physics of the ablation process.

The linear stability problem can be greatly simplified by an appropriate choice of the linearized equation of state. It is widely known that the most Rayleigh-Taylor unstable perturbations are incompressible. Furthermore, ablative stabilization is a convective process and is, therefore, independent of the equation of state. It follows that the essential physics of the instability can be captured by a simple incompressible flow model. The stability analysis proceeds in a standard manner. All perturbed quantities are written as $Q_1 = \tilde{Q}(y, t)\exp(ikx)$ and the system of equations describing the linear evolution of the perturbation assumes the following form:

$$\begin{aligned} (\partial_t + U_j \partial_y) \tilde{\rho}_j &= 0, \quad \rho_j (\partial_t + U_j \partial_y) \tilde{v}_{jx} = -ik \tilde{p}_j, \\ \rho_j (\partial_t + U_j \partial_y) \tilde{v}_{jy} + \tilde{\rho}_j \partial_t U_j &= -\partial_y \tilde{p}_j + \tilde{\rho}_j g, \\ ik \tilde{v}_{jx} + \partial_y \tilde{v}_{jy} &= 0, \end{aligned} \quad (4)$$

where the subscript j denotes the heavy fluid region ($j=h$) and the light fluid region ($j=l$) and $\partial_y = \partial/\partial y$, $\partial_t = \partial/\partial t$. The two regions are separated by an interface (the ablation front) that moves with the heavy fluid. The linear displacement of the interface $\tilde{\eta}(t)\exp(ikx)$ has to account for the heavy fluid ablative convection and can be described by the following integral equation:

$$\tilde{\eta}(t) = \int_{-\infty}^t \tilde{v}_{hy}[y_0(t'), t'] dt', \quad (5)$$

where $y_0(t') = \int_{t'}^t U_h(t'') dt''$ is the unperturbed trajectory of the fluid element that, at time t , has reached the ablation front. Since the heavy and light fluid extend to infinity and the instability is expected to be localized at the interface, the perturbation must vanish at $y \rightarrow \pm \infty$. A set of jump conditions relating the values of the physical quantities in the two regions can be derived by writing

the time derivative of any perturbed quantity \tilde{Q} at the ablation front as $\partial_t \tilde{Q} = -(Q_h - Q_l) \partial_t \tilde{\eta} \delta(y)$ and integrating the equations across the thin ablative layer. A short calculation yields

$$\begin{aligned} \tilde{v}_{hy} &= \tilde{v}_{ly}, \quad (\rho_h - \rho_l)(\partial_t \tilde{\eta} - \tilde{v}_{hy}) - U_h \tilde{\rho}_h + U_l \tilde{\rho}_l = 0, \\ \tilde{v}_{hx} - \tilde{v}_{lx} + ik \tilde{\eta}(U_h - U_l) &= 0, \\ \tilde{\rho}_h - \tilde{\rho}_l + \tilde{\rho}_h U_h^2 - \tilde{\rho}_l U_l^2 + g(\rho_h - \rho_l) \tilde{\eta} &= 0. \end{aligned} \quad (6)$$

The first of Eq. (6) follows directly from the incompressibility condition $\nabla \cdot \tilde{\mathbf{v}} = 0$. A better representation of the perturbation at the interface can be obtained by using an equation of state and calculating the jump in the energy [2]. However, when the flow is subsonic [$U_h^2, U_l^2 \ll p_h/\rho_h, p_l/\rho_l$], it is easy to show that the flow of internal energy across the interface has to be conserved and the incompressible result is recovered.

The solution of the linearized equation in the heavy fluid region (h) is greatly simplified by the following transformation variable: $y_h = y - \int_0^t U_h(t') dt'$. A straightforward calculation leads to the following form of the perturbed variables in region h :

$$\begin{aligned} \tilde{v}_{hy} &= \tilde{u}_h(t) \exp(-ky_h) + \tilde{a}(y_h), \quad \tilde{v}_{hx} = \frac{i}{k} \frac{\partial \tilde{v}_{hy}}{\partial y_h}, \\ \tilde{\rho}_h &= \tilde{\rho}_h(y_h), \quad \tilde{p}_h = -\frac{\rho_h}{k^2} \frac{\partial^2 \tilde{v}_{hy}}{\partial t \partial y_h}, \end{aligned} \quad (7)$$

where $\tilde{u}_h(t)$, $\tilde{\rho}_h(y_h)$, and $\tilde{a}(y_h)$ are arbitrary functions of t and y_h , and k is chosen to be positive ($k > 0$). In order to satisfy the boundary conditions, \tilde{a} and $\tilde{\rho}_h$ have to vanish at $y_h \rightarrow \infty$. Since $\lim_{t \rightarrow \infty} y_h = \infty$, it follows that \tilde{a} and

$\tilde{\rho}_h$ asymptotically vanish in time. In our asymptotic stability analysis, we neglect all the quantities that do not grow in time. Thus, we set $\tilde{a} = 0$ and $\tilde{\rho}_h = 0$. Furthermore, because of the incompressibility condition and negative flow velocity, $\tilde{\rho}_h = 0$ at all times.

We apply the same procedure to the light fluid region (l) and define the new coordinates $y_l = y - \int_0^t U_l(t') dt'$. The solution of the linearized equations in region l can be written in the following form:

$$\begin{aligned} \tilde{v}_{ly} &= \tilde{u}_l(t) \exp(ky_l) + \tilde{b}(y_l) + \tilde{c}(y_l) f(t), \\ \tilde{v}_{lx} &= \frac{i}{k} \frac{\partial \tilde{v}_{ly}}{\partial y_l}, \quad \tilde{\rho}_l = \tilde{\rho}_l(y_l), \quad \tilde{p}_l = -\frac{\rho_l}{k^2} \frac{\partial^2 \tilde{v}_{ly}}{\partial t \partial y_l}, \end{aligned} \quad (8)$$

where $\tilde{b}(y_l)$ and $\tilde{\rho}_l(y_l)$ are free functions of y_l that vanish at $y_l \rightarrow -\infty$, and $\tilde{u}_l(t)$ is an arbitrary function of t . The functions $\tilde{c}(y_l)$ and $f(t)$ satisfy the following differential equations:

$$\left[\frac{d^2}{dy_l^2} - k^2 \right] \tilde{c} + k^2 \frac{\tilde{\rho}_l}{\rho_l} = 0, \quad \frac{df}{dt} = G(t), \quad (9)$$

where

$$G(t) \equiv g(t) - \frac{\partial U_l}{\partial t}. \quad (10)$$

The next step is to recognize that, using Eqs. (7) in Eqs. (8), the interface equation can be rewritten in a differential form: $(\partial_t - kU_h) \tilde{\eta} = \tilde{v}_{hy}(y=0, t)$.

After substituting Eqs. (7) and (8) into the jump conditions [Eqs. (6)] and using the differential form of the interface equation, the following ordinary differential equation for $\tilde{\eta}(t)$ is derived:

$$(\partial_t - kU_l) G^{-1} \{ (\partial_t - kU_l) (\partial_t - kU_h) \tilde{\eta} + A [kU_l (\partial_t - kU_h) + kg] \tilde{\eta} \} - Ak^2 U_h \tilde{\eta} = 0, \quad (11)$$

where $A \equiv (\rho_h - \rho_l)/(\rho_h + \rho_l)$ is the Atwood number. For ICF applications, the appropriate ordering $U_h/U_l = \rho_l/\rho_h \sim 1 - A \ll 1$ and $g > \partial U_l/\partial t$. To lowest order in $1 - A$, the last term in Eq. (11) can be neglected, yielding

$$\{ (\partial_t - kU_l) (\partial_t - kU_h) + A [kU_l (\partial_t - kU_h) + kg] \} \tilde{\eta} = 0. \quad (12)$$

Equation (12) can be further simplified by using the ansatz

$$\tilde{\eta}(t) = \xi(t) \exp \left[\frac{3}{2} k \int_0^t U_h(t') dt' \right] \quad (13)$$

and by neglecting other terms of order $1 - A \ll 1$. After some straightforward manipulations, we obtain

$$\frac{d^2 \xi}{dt^2} + k \left[Ag - \frac{1}{2} \frac{dV_a}{dt} - \frac{1}{4} k V_a^2 \right] \xi = 0, \quad (14)$$

where g and V_a are functions of time with V_a the ablation velocity. Observe that, for steady equilibrium configurations, Eqs. (13) and (14) yield the normal mode solution for $\tilde{\eta} \sim \exp(\gamma t)$, with γ satisfying the dispersion relation

$$\gamma = \sqrt{(|kg|A) + \frac{1}{4} k^2 V_a^2} - \frac{3}{2} |kV_a|. \quad (15)$$

It is easy to recognize that the contribution of the second term under the square root is relevant only at very small

wavelengths, where the mode is already strongly stabilized by convection [the last term in Eq. (15)]. Neglecting such a term in Eqs. (14) and (15) would only cause a small shift of the cutoff wave number ($\Delta k_c/k_c = 1/9$) that is consistent with the order of magnitude of the previous approximations. After neglecting such a term, Eq. (15) reproduces the numerically derived growth rate of Ref. [3] with $\beta = 1.5$. Equations (13) and (14), which are valid for arbitrary unsteady configurations, can now be applied to the particular equilibrium obtained by temporally modulating the laser intensity. Consider a planar target of thickness d and density ρ_0 irradiated by a uniform laser beam. The periodically modulated laser intensity [$I(t) = I_0(1 + \Delta \sin \omega_0 t)$, $\Delta \leq 1$] induces an oscillating ablation pressure $P_a(t) = P_0(1 + \Delta_p \sin \omega_0 t)$ and ablation velocity $V_a(t) = V_{a0}(1 + \Delta_a \sin \omega_0 t)$ with $\Delta_p \lesssim \Delta$ and $\Delta_a \lesssim \Delta$. For simplicity, we assume that the ablation pressure and the ablation velocity are directly proportional to the laser intensity and the ablation process develops on a very slow time scale compared to an oscillation period and the sound transit time through the target [$V_a \ll c_s$, c_s is the sound speed]. Although the scaling $V_a \sim \sqrt{I} \sim [1 + \Delta \sin(\omega_0 t)]^{1/2}$ is more appropriate than a simple linear dependence, the numerical simulations show that the ab-

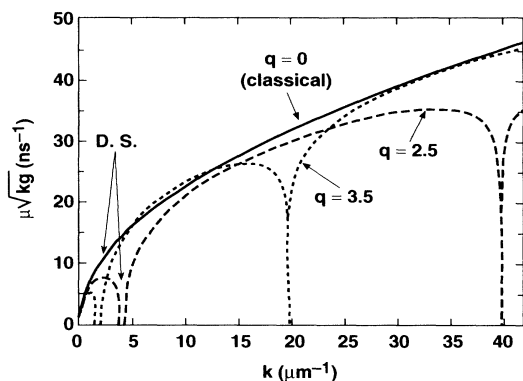


FIG. 1. Plot of the instability drive term μ , versus the mode wave number k for modulated ($q \neq 0$) and unmodulated ($q = 0$) laser intensity, assuming $d = 20 \mu\text{m}$, $g_0 = 5 \times 10^{15} \text{ cm/s}^2$, the Atwood number $A = 1$, $\langle V_a \rangle = 7 \times 10^4 \text{ cm/s}$, $T_0 = 0.3 \text{ ns}$, and $\phi = 0$.

lation velocity is almost insensitive to the oscillations in the laser intensity ($\Delta_a \ll 1$) and $V_a \approx V_{a0}$. I_0 and P_0 are two slowly varying functions of time [$V_a/d < (1/I_0)dI_0/dt = (1/P_0)dP_0/dt \ll \omega_0 \sim c_s/d$]. A simple estimate of the acceleration of the ablation front can be derived by solving the one-dimensional compressible fluid equations of Ref. [6] for a target accelerated by the ablation pressure. The result is

$$g(t) = -\frac{dV_a}{dt} - L^{-1} \left\{ \coth \left[\frac{s}{c_s} (d - \bar{y}_a) \right] \frac{s \hat{p}_a(s)}{\rho_0 c_s} \right\}, \quad (16)$$

where L^{-1} denotes the inverse Laplace transform, s is the Laplace variable, and $\hat{p}_a(s)$ is the Laplace transform of the ablation pressure. The quantity $\bar{y}_a = \int_0^t V_a(t') dt'$ is the position of the ablation front in the Lagrangian frame of the moving target. In deriving Eq. (16), the slow ablation time scale ($\sim d/V_a$) has been treated as an independent variable. A simple expression for $g(t)$ can be derived in the asymptotic limit $d/V_a > t \gg d/c_s$, yielding

$$g(t) = -g_0 [1 + \alpha \sin \omega_0 t + \epsilon \cos \omega_0 t], \quad (17)$$

where $g_0 \equiv P_0/\rho_0 d_a$, $\alpha \equiv \Delta_p(\omega_0 d_a/c_s) \cot(\omega_0 d_a/c_s)$, and $\epsilon = V_{a0} \Delta_a \omega_0/g_0$, $d_a = d - \bar{y}_a$. A more accurate estimate of $g(t)$ (and of the parameters g_0 , α , and ϵ) can be obtained by using a one-dimensional code. Later in this Letter we will use the one-dimensional hydrodynamic code LILAC [7] to derive g_0 , α , and ϵ . However, Eq. (17) gives some physical insight into the relevant quantities that affect the oscillation amplitude in the target acceleration. In particular, large oscillations can be achieved for values of the modulation period shorter than the sound transit time through the target ($T_0 \equiv 2\pi/\omega_0 < d/c_s$). Before proceeding further, it is important to define the range of validity of the stability model for the prescribed equilibrium. The oscillations in the ablation pressure propagate inside the target at the sound speed. Thus, the equilibrium parameters can be considered as uniform over a distance $\Delta y < c_s T_0$. The stability analysis, carried out for a uniform

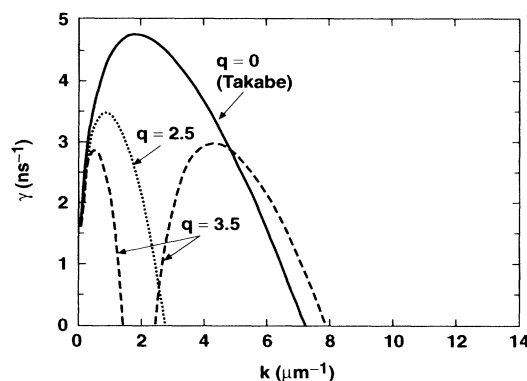


FIG. 2. Plot of the instability growth rate versus the mode wave number k for modulated ($q \neq 0$) and unmodulated ($q = 0$) laser intensity, assuming the same equilibrium parameters as in Fig. 1.

semi-infinite medium, can be applied to perturbations with sufficiently short wavelength $k\Delta y > 1$. It follows that a necessary condition for the validity of the stability model is $kc_s T_0 \gg 1$. For such wavelengths, Eq. (17) can be used in Eq. (14) to derive the function $\xi(t)$. Thus, Eq. (14) can be written in the following form:

$$\frac{d^2 \xi}{dt^2} - \gamma_c^2 [1 + q \sin(\omega_0 t + \phi)] \xi = 0, \quad (18)$$

where $\gamma_c = \sqrt{A|kg_0|}$ is the classical growth rate, $q = \sqrt{\alpha^2 + 9\epsilon^2}/4$, and $\phi = \tan^{-1}(3\epsilon/2\alpha)$. Notice that Eq. (18) is a Mathieu equation, whose solution has the form $\xi(t) = \sigma(t) \exp(\mu t)$, with $\sigma(t)$ being periodic with period ω_0 . Using Eq. (13), the growth rate of the instability can be easily derived,

$$\gamma = -k\beta \frac{1}{T_0} \int_0^{T_0} V_a(t') dt' + \mu, \quad (19)$$

where $\beta = 1.5$ for the simplified stability model. However, when Eq. (19) is compared to the Takabe formula, we let $\beta = \beta^T = 3-4$. In order to find μ , one needs to numerically solve Eq. (18) for one period of oscillation. Figure 1 shows the parameter μ , plotted versus the wave number k , for the following equilibrium parameters $d = 20 \mu\text{m}$, $g_0 = 5 \times 10^{15} \text{ cm/s}^2$, $A = 1$, $\langle V_a \rangle = 7 \times 10^4 \text{ cm/s}$, $c_s = 10^6 \text{ cm/s}$, $T_0 = 0.3 \times 10^{-9} \text{ s}$, $\phi = 0$, and $q = 0, 2.5$, and 3.5 . The validity of the stability model requires $\lambda = 2\pi/k \ll 20 \mu\text{m}$. For any value of q and ω_0 , it is possible to identify intervals of the k axis where $\text{Re}[\mu] = 0$. We denote such intervals as dynamically stabilized (DS) regions, and we emphasize the importance of ablative convection [see Eq. (19)] at shorter wavelengths. According to Eqs. (1) and (19), the short wavelength modes are stabilized by convection and the cutoff wave number is $k_c = gA/\beta^2 V_a^2$. It follows that an efficient dynamic stabilization can be achieved by choosing values of q and ω_0 that cause the first DS region to be located inside the interval $0 < k < k_c$. In Fig. 2, the growth rates derived from Eq. (19) for $q = 0, 2.5$, and 3.5 and $\beta = 3.5$ (as given by Takabe *et*

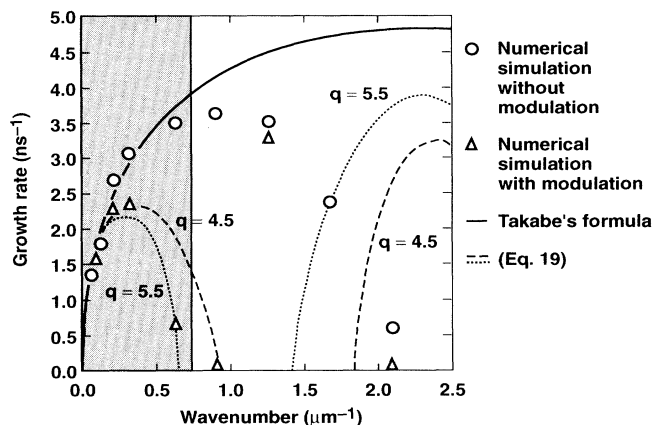


FIG. 3. Comparison of the growth rate obtained from numerical simulations (with modulation Δ and without modulation \circ) and the modified Eq. (19). Here, $d = 18 \mu\text{m}$, $g_0 = 4.5 \times 10^{15} \text{ cm/s}^2$, $\langle V_a \rangle = 7 \times 10^4 \text{ cm/s}$, $T_0 = 0.3 \text{ ns}$, $\phi = 0$, $A = 1$, $\beta = 3$, $\theta\delta = 1.5 \times 10^{-5} \text{ cm}$, $q = 5.5$ (dotted), $\beta = 4$, $\theta\delta = 0.3 \times 10^{-5} \text{ cm}$, $q = 4.5$ (dashed). The solid line represents the Takabe formula and the shaded area represents the region with $k\delta \lesssim 1$.

al. [3]) are shown. Observe that as q increases, a better stabilization is induced at longer wavelengths, but shorter wavelengths can be destabilized ($q = 3.5$). This short wavelength instability is driven by the oscillations in the acceleration, with the perturbation having the characteristic structure of an oscillatory mode with an exponentially increasing amplitude. For convenience, we denote these short wavelength modes as "parametric instabilities." Furthermore, when the mode wavelength is smaller than the density gradient scale length [$\delta = |(1/\rho)dp/dy|^{-1}$], the sharp boundary model is not valid and Eq. (19) cannot be used.

The results of the analytic theory have been compared with two-dimensional simulations obtained using the code ORCHID [8]. We have considered an 18- μm CH planar target irradiated by a uniform laser beam of wavelength 1.06 μm . The laser intensity is modulated in time with a period of 0.3 ns. The modulation amplitude is 100%, and the flat-top average intensity is 50 TW/cm². For an accurate comparison with the analytic stability theory, we derive the equilibrium parameters g , $\langle V_a \rangle$, and q , from the one-dimensional code LILAC [7]. The result is $g = 4.5 \times 10^{15} \text{ cm/s}^2$, $\langle V_a \rangle = 7 \times 10^4 \text{ cm/s}$, $\delta = 1.5$ to 2 μm , $\phi = 0$, and $q = 3.5$ to 5.5. In the two-dimensional simulation, an initial single wavelength perturbation evolves for 3 ns. Because of the short modulation period, the simulation shows no significant change in the foil isentrope with respect to the unmodulated case. Figure 3 shows a comparison between the linear growth rate derived from the simulation, with the one given by Eq. (19). Three regions of the k axis can be identified: (1) The long wavelength region with $k < 0.2 \mu\text{m}^{-1}$, where the growth rate is virtually insensitive to the modulation of the laser intensity and very close to the classical value. (2) The intermediate wavelength region with $0.2 < k < 1$. For these values

of the wave number, the dynamic stabilization is particularly effective. Observe that for $\lambda = 2\pi/k \approx 7 \mu\text{m}$, the mode is completely stabilized. (3) The short wavelength region is defined as having a wave number $k > 1$. In this region $k\delta > 1$ and the effect of finite density-gradient scale length cannot be neglected. Notice that the simulation shows the presence of an unstable mode with wavelength $\lambda \approx 5 \mu\text{m}$. Using Eq. (19) beyond its limit of validity ($k\delta < 1$) and dividing γ_c^2 by $1 + \theta k\delta$ with $\theta < 1$, we would predict the existence of parametric instabilities at shorter wavelengths (Fig. 3). However, the structure of the perturbation observed in the numerical simulation does not clearly show the characteristics of a parametric instability. Furthermore, the cutoff wave number observed in the numerical simulation (with or without laser intensity modulation) is much shorter than the one predicted by Eqs. (1) and (19). The stability of very short wavelength perturbations needs further investigation to determine an accurate value of the cutoff wave number.

The dynamic stabilization of the Rayleigh-Taylor instability in ICF targets was first observed in numerical simulations by Boris [9]. In this Letter we have shown the derivation of the linear stability theory for unsteady ablation fronts and the conditions for the dynamic stabilization of the ablative Rayleigh-Taylor instability. The growth rate of the instability has been calculated for a sinusoidal modulation of the laser intensity. It is shown that an appropriate modulation frequency and amplitude can stabilize a large portion of the unstable spectrum and significantly reduce the maximum growth rate.

The authors would like to thank Professor Al Simon for useful discussions. This work was supported by the U.S. Department of Energy Office of Inertial Confinement Fusion under Cooperative Agreement No. DE-FC03-92SF19460, the University of Rochester, and the New York State Energy Research and Development Authority.

- [1] Lord Rayleigh, *Scientific Papers* (Cambridge University Press, Cambridge, England, 1900), Vol. II, p. 200.
- [2] S. Bodner, *Phys. Rev. Lett.* **33**, 761 (1974).
- [3] H. Takabe, K. Mima, L. Montierth, and R. L. Morse, *Phys. Fluids* **28**, 3676 (1985).
- [4] H. J. Kull and S. I. Anisimov, *Phys. Fluids* **29**, 2067 (1986).
- [5] A. B. Bud'ko and M. A. Liberman, *Phys. Rev. Lett.* **68**, 178 (1992).
- [6] N. Rostoker and H. Tahsiri, *Comments Plasma Phys. Controlled Fusion* **3**, 39 (1977).
- [7] E. Goldman, Laboratory for Laser Energetics Report No. 16, 1973 (unpublished); J. Delettrez and E. B. Goldman, Laboratory for Laser Energetics Report No. 36 1976 (unpublished).
- [8] R. L. McCrory and C. P. Verdon, in *Computer Applications in Plasma Science and Engineering*, edited by Adam T. Drobot (Springer-Verlag, New York, 1991), pp. 291-325.
- [9] J. P. Boris, *Comments Plasma Phys. Controlled Fusion* **3**, 1 (1977).